



**HAL**  
open science

## Distribution of duricrusted bauxites and laterites on the Bamiléké plateau (West Cameroon): Constraints from GIS mapping and geochemistry

Mathieu Nouazi Momo, Martin Yemefack, Paul Tematio, Anicet Beauvais,  
Jean-Paul Ambrosi

### ► To cite this version:

Mathieu Nouazi Momo, Martin Yemefack, Paul Tematio, Anicet Beauvais, Jean-Paul Ambrosi. Distribution of duricrusted bauxites and laterites on the Bamiléké plateau (West Cameroon): Constraints from GIS mapping and geochemistry. *CATENA*, 2016, 140, pp.15-23. 10.1016/j.catena.2016.01.010 . ird-01419953

**HAL Id: ird-01419953**

**<https://ird.hal.science/ird-01419953>**

Submitted on 20 Dec 2016

**HAL** is a multi-disciplinary open access archive for the deposit and dissemination of scientific research documents, whether they are published or not. The documents may come from teaching and research institutions in France or abroad, or from public or private research centers.

L'archive ouverte pluridisciplinaire **HAL**, est destinée au dépôt et à la diffusion de documents scientifiques de niveau recherche, publiés ou non, émanant des établissements d'enseignement et de recherche français ou étrangers, des laboratoires publics ou privés.

1           **Spatial distribution of bauxitic duricrusted laterites on the Bamiléké**  
2           **plateau (West Cameroon): constrained GIS mapping and geochemistry**

3           Mathieu NOUAZI MOMO\*<sup>1</sup>, Martin YEMEFACK<sup>2,3</sup>, Paul TEMATIO<sup>1</sup>, Anicet BEAUVAIS<sup>4</sup>, Jean-Paul AMBROSI<sup>4</sup>  
4

5           <sup>1</sup> University of Dschang, Faculty of Science, Department of Earth Science, PO Box 67, Dschang, Cameroon.

6           <sup>2</sup> Institute of Agricultural Research for Development (IRAD), PO Box 2067, Yaoundé, Cameroon,

7           <sup>3</sup> International Institute of Tropical Agriculture (IITA), ASB Partnership REALU Project, PO Box 2008 (Messa)  
8           Yaoundé, Cameroon.

9           <sup>4</sup> Aix-Marseille Université, CNRS, IRD, CEREGE UM34, 13545 Aix-en-Provence, France.

10

11           \*Corresponding author: Tel. (237) 695650828; Email: [nouazimat@yahoo.fr](mailto:nouazimat@yahoo.fr) & [nouazi@cerege.fr](mailto:nouazi@cerege.fr)

12           **Running Title:** Bauxitic duricrusts on the Bamiléké Plateau

13

14 **Abstract**

15 Estimation of the mineral resources potential is an important issue for most of developing countries. The  
16 spatial distribution of lateritic landsurfaces and bauxite on the Bamiléké plateau (West Cameroon) has  
17 been investigated with a Boolean modeling process into a GIS environment on the basis of geological  
18 constraints namely elevation, rock types, landscape morphology and soil types. Field observation and  
19 SRTM (Shuttle Radar Topographic Mission) data allowed the differentiation of two lateritic surfaces  
20 separated by a minimum altitude difference of about 60 m. These surfaces constrained by favorable rock  
21 types, slope steepness and soil types provided a potential lateritic bauxitic area of 381 km<sup>2</sup> (17.2% of the  
22 total study site), which matches the current bauxitic areas and evidences a large non-explored area in the  
23 north of the study site. Field validation and the integration of legacy spatial data resulted in an area of  
24 60.1 km<sup>2</sup> for potential bauxitic ores, i.e. obviously duricrusted landsurfaces (with 47.8 km<sup>2</sup> in the upper  
25 surface and 12.3 km<sup>2</sup> in the lower surface). Geochemical data (mostly Al<sub>2</sub>O<sub>3</sub> wt.%) obtained from  
26 duricrust samples were treated by geostatistical methods and classical kriging interpolation to  
27 discriminate between bauxitic and ferruginous laterites. This highlighted a geochemical trend from higher  
28 alumina values on the upper surface (40-66 wt.%) to lower values on the lower surface (13-44 wt.%).  
29 Finally, our study documents two indurated lateritic surfaces arranged in a staircase manner and having  
30 different geochemical characteristics. The total bauxitic-rich surface is distributed in five different spots  
31 throughout the study area and covers 56.2 km<sup>2</sup>, while ferruginous laterites occupy a spot of 3.9 km<sup>2</sup>. GIS  
32 mapping approach of lateritic landsurfaces, accounting for reliable constraints, might be promising for  
33 larger scale investigations of mineral resources in developing Countries.

34

35 Keywords: Bauxite; Boolean modeling; Kriging; Bamiléké plateau; Cameroon

36

## 37 **1. Introduction**

38 Many Third World Countries rely mainly on their natural resources to sustain their economic  
39 development. In Cameroon, the exploitation of mineral resources has traditionally been a significant  
40 component of the economy (Ntép Gweth, 2009). However, knowledge on the real potential of these  
41 resources is generally limited by a lack of geo-exploration tool required for their reliable and  
42 comprehensive assessment and classification at the national-wide level. In this country, the most  
43 widespread ore deposits are lateritic bauxites, representing the 6<sup>th</sup> reserve in the world. Bauxites occur in  
44 the Adamaoua and Western regions, and have been previously studied by many authors (Eno Belinga,  
45 1968; Eno Belinga, 1972; Hiéronymus, 1973; Momo Nouazi et al., 2012; Morin, 1985; Nicolas and Eno  
46 Belinga, 1969; Nyobe, 1987) using classical approaches of field survey and laboratory analyses.  
47 Nowadays, GIS and remote sensing tools permit more accurate mapping of such resources by integrating  
48 favorable geological constraints in a GIS-based model.

49 Our study aimed at satisfying the practical need for supporting bauxite exploration in Cameroon  
50 with up-to-date maps, by defining the relation between bauxitic deposits and their geological  
51 environment. For this purpose, we used a GIS-modeling approach, based on a well-established procedure  
52 previously tested in several studies on mineral potential assessment (Bonham-Carter, 1994; Boroushaki  
53 and Malczewski, 2008; Carranza, 2002; Carranza, 2009; Carranza et al., 1999; Carranza et al., 2008;  
54 Cheng and Agterberg, 1999; Guha et al., 2013; Harris et al., 2008; Harris et al., 2001; Robinove, 1989;  
55 Thiart and De Wit, 2000; Thole et al., 1979; Varnes, 1974; Zadeh, 1965). The approach deals with GIS-  
56 based geologically constrained mineral potential mapping, a multistage strategy for delineating  
57 mineralized zones (Reeves et al., 1990). Multivariate and multisource geo-exploration datasets were  
58 combined to enhance favorable geologic features indicative of mineral deposit (Bonham-Carter, 1994;  
59 Hodgson, 1990). Our interest was thus to know via the Boolean model of Varnes (1974) and Robinove  
60 (1989), whether the spatial criteria linked to the genetic environment and landscape distribution of

61 bauxites can be used to define predictive map of bauxite occurrence for further field exploration and  
62 geochemical survey.

63

## 64 **2. Physiography of the study area**

65 The study site lies between longitudes 09°56'-10°20'E, and latitudes 05°18'-5°45'N and covers  
66 an area of 2209 km<sup>2</sup> within the Bamiléké plateau extending between 09°44'-10°33'E, and 04°10'-  
67 05°56'N in West Cameroon (Figs. 1A and B). The main morphological features of this area is the Mount  
68 Bambouto, culminating at the altitude of 2725 m (Fig. 1B), which is the third most important and highest  
69 volcano of the Cameroon Volcanic Line (Déruelle et al., 1991). It covers the southern part of the West  
70 Cameroon highland between the Bamoun plateau in the east, the Grassfields in the north and the Mbô  
71 plain in the south and west.

72 The climate of the Bamiléké plateau is sub-equatorial, influenced by high altitudes, with 1600-  
73 2000 mm mean annual rainfall and 18°C-20°C for the mean annual temperature.

74 The Cameroon Volcanic Line consists of a wide Cenozoic volcanic complex extruded on the  
75 Neoproterozoic Panafrican granito-gneissic basement, which is also intruded by mafic and felsic plutons  
76 (Kwekam et al., 2010). The volcanic complex is known to be the parent material for the plateau Bamiléké  
77 bauxites. The new <sup>40</sup>K-<sup>40</sup>Ar geochronological data showed three main periods of volcanic activity  
78 extending from the Miocene (Burdigalian) (Marzoli et al., 1999) to the Pliocene (Nkouathio, 2006), and  
79 uncommon lava spots extending up to ~0.5 My (Kagou Dongmo et al., 2010). Lavas geochemistry shows  
80 a trend extending from basanites to trachytes or phonolytes.

81

## 82 **3. Methods**

### 83 3.1. Conceptual model of bauxite occurrence

84 A conceptual and exploration model for evaluating the bauxite potential of the Bamiléké Plateau  
85 was built based on geological criteria (Carranza, 2002; De Araújo and Macedo, 2002; Hodgson, 1990;

86 Reeves et al., 1990). Amongst the operators used for examining the spatial association of geological  
87 features is the Boolean model, which is based on a reclassification of the input maps into only two classes  
88 (Bonham-Carter, 1994; Carranza et al., 2008; Harris et al., 2001; Robinove, 1989; Thiart and De Wit,  
89 2000; Varnes, 1974), i.e., the maximum and minimum evidential score classes (0 or 1). Reclassified maps  
90 are combined logically according to a set of steps so-called inference network (Fig. 2), which reflects the  
91 inter-relationships of processes controlling the occurrence of a geo-object and the spatial features  
92 indicating the presence of this geo-object (Carranza, 2002; Carranza, 2009). Finally, the output of  
93 combined evidential maps via Boolean logic modeling is a two class map; the first class represents  
94 locations where all of the prospective recognition criteria are satisfied, whilst the second class represents  
95 locations where at least one is unsatisfied (Carranza, 2009).

96 The study was carried out with ILWIS GIS software (ITC ILWIS Unit, 2001) using a three step  
97 methodology including: (1) gathering spatial data into a GIS, (2) extracting spatial evidential data and  
98 creating derivative maps to be used as spatial evidence of bauxite mineralization, (3) integrating the  
99 spatial evidence map to create bauxitic potential map and validating the predictive map (Bonham-Carter,  
100 1994).

101

### 102 3.2. Analysis of constraints

103 In our study, the criteria or constraints from the rock types, landscape morphology (elevation  
104 ranges and slopes), and soil types were defined and linked to delineate favorable zones on the Bamiléké  
105 Plateau. These zones are potentially duricrusted landsurfaces areas with alumina-rich surface materials,  
106 which are characterized by deep and extremely leached soils (Hiéronymus, 1973; Momo Nouazi et al.,  
107 2012; Nyobe, 1987).

108 Lateritic bauxites are known to form mainly by chemical weathering of rocks in which low silica  
109 content favors crystallization of gibbsite instead of kaolinite (Tardy, 1993). However, many other studies  
110 have also described bauxite formation from a variety of parent materials including basic and acid rocks

111 (Bildgen, 1973; Boulangé, 1984; Boulangé et al., 1997; Boulangé et al., 1996; Boulangé and Colin, 1994;  
112 Chardon et al., 2006; Eno Belinga, 1972; Momo Nouazi et al., 2012; Soler and Lasaga, 2000).  
113 Meanwhile, the geological substratum is an important factor contributing to the preservation of lateritic  
114 bauxites from surface stripping (Boulangé, 1984). On the Bamiléké plateau, a variety of rocks derived  
115 from complex magmatic and metamorphic events exist (Dumort, 1968; Kagou Dongmo et al., 2010;  
116 Kwekam et al., 2010; Nkouathio et al., 2008), but the bauxites are formed exclusively upon volcanic  
117 rocks (Momo Nouazi et al., 2012; Morin, 1985; Nyobe, 1987).

118 Bauxitic laterites generally occur on high elevation, low relief planation landsurface remnants  
119 lying on flat or gently sloped surfaces (Grandin and Thiry, 1983; Chardon et al., 2006; Beauvais and  
120 Chardon, 2013). These morphological characteristics allow localizing bauxitic laterites from altitudinal  
121 levels and slope distribution (Riis and Fjeldskaar, 1992).

122 Bauxitic laterites are developed under a tropical climate that favors deep rock weathering and the  
123 development in soils of a thick B-horizon resulting from lixiviation process (Boulangé and Colin, 1994;  
124 Grandin and Thiry, 1983; Maignien, 1966; Pedro, 1968; Tardy, 1993). Commonly, bauxites described on  
125 well-preserved landsurfaces show thickness extending up to 20 and 30 m (Grandin and Thiry, 1983;  
126 Segalen, 1967). The presence or absence of the B-horizon in soils was used to determine potential areas  
127 of bauxite development in the study area.

128

## 129 **4. Results**

### 130 4.1. Favorable constraints

#### 131 *4.1.1. Favorable rock types*

132 Within the study site, volcanic rocks cover 64% of the total surface (Fig. 3A), comprising mainly  
133 basalts (64%), trachytes (28%) and ignimbrites (6%), which have been formed since 19 My covering an  
134 area of 1406 km<sup>2</sup> (Marzoli et al., 1999; Nkouathio et al., 2008). All these volcanic rocks currently show  
135 evidence of deep weathering process (Tematio et al., 2004). Phonolites and volcanic ashes cover limited

136 areas (~1%) on the study site. These recent volcanic rocks range from 4 My for phonolites (Nkouathio et  
137 al., 2008) to 0.48 My for volcanic ashes (Kagou Dongmo et al., 2010). The phonolites are found on  
138 elevated dykes with no evidence of weathering. Volcanic ashes are very little altered exhibiting a very  
139 thin non-differentiated profile (Tsopjio Jiomeneck et al., 2011). Taking into account all these data,  
140 basalts, trachytes and ignimbrites are rock types with potential to control bauxite occurrences in the study  
141 area.

#### 142 *4.1.2. Favorable morphological features: elevation and slope*

143 On the Bamiléké plateau, legacy data and field observations have contributed to differentiate two  
144 lateritic surfaces with minimum elevation of 1520 and 1580 m for the lower and the upper surface,  
145 respectively (Fig. 3B). The 60 m height difference (Dh; Fig. 4) is a lithologically controlled feature  
146 marked by flow scarps separating two types of volcanic materials. These are reported on the central and  
147 the western part of the study site (Fig. 4) as a limit between the Mount Bambouto lava and the  
148 surrounding shield (Nkouathio et al., 2008); and on the southeastern part by the Bangam flow scarp. The  
149 lower surface is an undulated low relief landscape with few interfluves culminating up to about 1580 m,  
150 corresponding mainly to the Doumbouo-Fokoué area (Fig. 3B; Fig. 4) between large remnants of the  
151 upper surface (Fig. 3B). The upper surface includes the so called Fongo-Tongo deposit, the Loung deposit  
152 and the Bangam deposit (Fig. 3B; Fig. 4) and a large unexplored area in the northern part of the study site  
153 (Fig. 3B), whose the maximum altitude is not actually well defined although laterites have been described  
154 up to about 1900 m.

155 Remnants of bauxitic surfaces on the Bamiléké plateau are most often highly dissected due to the  
156 combined effects of tectonic uplift, climate and drainage pattern (Morin, 1985), and are incised by steep  
157 valleys. Landscape dissection results in two morphological features related to different incision stages.  
158 The first one corresponds to isolated gently sloping interfluves (0 to 5°; Fig. 3C), which are covered by  
159 continuous duricrusted laterites (Fig. 5A) and limited by steep slopes up to 76° (Fig. 5B). The second  
160 feature corresponds to widespread elongated interfluves with convex summits showing slope classes



161 ranging from 0 and 15° (Fig. 3C). Well-preserved duricrusts occur on the lowest slopes, but are stripped  
162 on increasing slopes steepness. This is obvious on a sequence at Doumbouo-Fokoué showing continuous  
163 duricrust on the top, discontinuous duricrust on summit shoulder, and gravelly horizon on 15° slopes  
164 marking the lower topographic limit of the lateritic surface (Fig. 5C). Landform units and slope classes  
165 derived from SRTM (Shuttle Radar Topographic Mission) data were thus potential morphological  
166 features for mapping bauxitic deposits. The favorable elevation ranges delineate a surface of 685 km<sup>2</sup> and  
167 223 km<sup>2</sup> on the upper surface and lower surface, respectively (Fig. 3B). Favorable sloping land surface  
168 covers a total surface of 1702 km<sup>2</sup> with slopes ranging between 5-15° over a surface of 1176 km<sup>2</sup> (Fig.  
169 3C).

#### 170 *4.1.3. Favorable soil classes*

171 Three major soil classes are recorded in the area: andosols, andic-ferralitic soils and ferralitic soils  
172 (Tematio, 2005; Tematio et al., 2009; Tematio et al., 2004) corresponding respectively to andosols,  
173 acrisols and ferralsols of the World Reference Base for soil classification (FAO-ISRIC, 2006; Jones et al.,  
174 2013). These soils form a toposequence extending from andosols at the upper part of the Bambouto  
175 volcano, to acrisols at the middle, and to ferralsols in lower part (Fig. 3D). The B-horizon is well  
176 developed except in the andosols of high altitudes where cool climate prevents clay formation and instead  
177 favors organo-metal complexes embedding Al and Fe (Tematio, 2005). This results in the development of  
178 a thick organic horizon lying in most cases directly on the bedrock. These andosols are associated on  
179 either side of the Mont Bambouto caldera edge with lithosols, which were strongly eroded and reworked  
180 out by numerous landslides occurring from the top of the volcano to about 600 m altitudes westward.  
181 Accordingly, only ferralsols and acrisols, which cover 1645 and 131 km<sup>2</sup>, respectively, are considered for  
182 the modeling process.

183

#### 184 *4.2. Mapping the bauxitic potential*

185 Spatial evidences of bauxitic potential were constrained successively from different geological  
186 features as described in section 3. First, the maps constrained by elevation and lithology displayed two  
187 main areas of bauxite potential, i.e., the northern area made up mainly of the upper surface and the  
188 southern area made up mainly of the lower surface (Fig. 6A). The total potential surface at this stage  
189 covers 682 km<sup>2</sup> (538 km<sup>2</sup> and 144 km<sup>2</sup> for the upper and the lower surface, respectively). This surface was  
190 further constrained with the favorable soil classes, and the resulting surface showed 422 km<sup>2</sup> with 291  
191 km<sup>2</sup> for the upper surface and 131 km<sup>2</sup> for the lower surface. The spatial distribution pattern remains the  
192 same as the first potential map, except that the upper surface was reduced in the northern part of the study  
193 site (Fig. 6B).

194 Finally, the map derived from the altitudes, lithology, and soils was further constrained by the slope  
195 map that resulted in a predictive bauxitic map characterized by large blank areas with dissected pattern  
196 (Fig. 6C) corresponding to slopes ranging from 15 to 76°. The total potential surface is 381 km<sup>2</sup>, i.e.  
197 17.2% of the total studied zone. The slopes of 5-15° is the most represented (76%), showing that the  
198 dominant morphological features for bauxite occurrence are the convex shaped summit of elongated  
199 interfluves.

200

#### 201 4.3. Validation of the predictive bauxitic laterites map

202 As shown in the inference network of Fig. 2, the map of the predictive bauxitic areas was an  
203 intermediate step of the modeling process. Comparing this map with data from previous studies and field  
204 campaigns was the final step to validate the efficiency of the model for evaluating the accuracy of bauxite  
205 mapping. The validation consisted in (i) gathering data from different sources to precisely delineate  
206 lateritic duricrusts, and (ii) integrating geochemical data interpolated by kriging to differentiate between  
207 ferruginous and bauxitic laterites. The first step in validating the output map was carried out by a rough  
208 comparison between the predictive map and the areas with previously studied bauxites deposits such as  
209 Fongo-Tongo, Djeu and Loung-Ndoh (Morin, 1985; Nyobe, 1987), Doumbouo-Fokoué (Hiéronymus,

210 1973; Momo Nouazi et al., 2012; Morin, 1985), and Bangam (Hiéronymus, 1973; Morin, 1985). The  
211 predictive map perfectly matches these areas and highlights a large northern site for which legacy data are  
212 still lacking as shown on the figure 6C. Upon validation process, the predictive map delineate a surface of  
213 60.1 km<sup>2</sup> of lateritic duricrusts on the Bamiléké plateau with 47.8 km<sup>2</sup> for the upper surface and 12.3 km<sup>2</sup>  
214 for the lower surface (Fig. 6D).

215         The second step aimed at differentiating between bauxitic laterites and ferruginous laterites. For  
216 this purpose, a total of 65 samples randomly distributed in the study area were collected, analyzed for  
217 geochemical data (Table. 1) and used for geostatistical analyses. The process of interpolation carried out  
218 in this step consisted in determining the distribution of alumina weight percentage on regularly distributed  
219 points (pixels) from randomly distributed analytical point values. The output of point interpolation is a  
220 raster map, whose pixel values are calculated by interpolation from input point values. The kriging  
221 method with a minimum mean interpolation error is currently used (Theodossiou and Latinopoulos,  
222 2006). In this study, the kriging process established a spatial correlation between the spatial input values  
223 at an optimal lag distance of 1 km. A spherical model fitted to the semi-variogram from this correlation  
224 was used as interpolation function. The figure 7 shows the kriging map differentiating three main  
225 geochemical areas. The first area is characterized by highest alumina values, confined on the upper  
226 surface (comprising localities of Fongo-Tongo, Djeu, Loung-Ndoh and Bangam). The geochemical trends  
227 are represented with alumina values decreasing from Fongo-Tongo to Djeu on the western part of the  
228 lateritic map, and on the eastern part with a slight increasing trend toward the SE (Bangam). These areas  
229 display interpolated alumina values extending from 44 up to 66 wt.% Al<sub>2</sub>O<sub>3</sub>. The second area is  
230 delineated in the southern part of the lower surface at Fokoué and Sa, where alumina values extend from  
231 40 to 44 wt.% Al<sub>2</sub>O<sub>3</sub> with a slight decrease northward (Fig. 7). The third area is confined to the  
232 Doumbouo region where ferruginous laterites are characterized by alumina content less than 40 wt.%,  
233 varying from 39 to 13 wt.% Al<sub>2</sub>O<sub>3</sub>. The total bauxitic-rich surface of the Bamiléké plateau is then of 56.2  
234 km<sup>2</sup>, while ferruginous laterites cover a surface of 3.9 km<sup>2</sup>.

## 235 5. Discussion

### 236 5.1. Spatial features evidence and predictive map of bauxite potential

237 The Boolean model applied in this study has resulted in an 82.8% reduction in the potential  
238 bauxite area to be considered. The predictive map has indicated that the bauxite potential covers 17.2% of  
239 the total study area, that perfectly matches known areas of bauxite deposits as derived from previous  
240 studies on the Bamiléké plateau (Hiéronymus, 1973; Momo Nouazi et al., 2012; Morin, 1985; Nyobe,  
241 1987). Out of the 17.2% bauxite potential from the predictive map, the total confirmed bauxitic area of  
242 the Bamiléké plateau derived from validation steps only covers about 3% of the total investigated area  
243 (56.1 km<sup>2</sup>). This reduced bauxitic surface can be explained by (i) the advanced stage of bauxitic  
244 landsurface dismantling (Momo Nouazi et al., 2012), which induces the total stripping of duricrust on  
245 interfluves with favorable genetic characteristics (rock and soil) and favorable morphological criteria; and  
246 (ii) the flat and gently sloped areas in the northern part of the predictive map covered by unaltered basaltic  
247 and trachytic flows. This methodology allows a regional scale evaluation of lateritic bauxites by  
248 highlighting the low preservation and increasing dismantling of these lateritic surfaces, which had already  
249 been noticed all over the remnants of the planation surfaces (see Momo-Nouazi et al., 2012). The criteria  
250 used in this study are quite similar to those used by Carranza (2002) for determining the predictive map of  
251 nickeliferous-laterites of the Isabel area in Philippines. The resulting map demonstrated the reliability of  
252 the method in large areas with a limited number of mineral prospects. It is thus a relatively effective,  
253 rapid, and cheap approach, which can be applied to assess a large number of mineral potential as  
254 described by Bonham-Carter (1994). It can then be considered as a promising approach applicable to  
255 other bauxitic regions of Cameroon such as the Adamaoua bauxitic landsurfaces with wide duricrusted  
256 and gently sloped plateaus ( $\leq 2^\circ$ ) developed on volcanic rocks (Eno Belinga, 1966; Vicat and Bilong,  
257 1998) for a larger scale spatial regionalization.

258

### 259 5.2. Bauxites of the Bamiléké plateau and its economic potential

260 Bauxites of the Bamiléké plateau are distributed in five main spots named Bangam, Doumbouo-  
261 Fokoué, Fongo-Tongo, Loung-Ndoh and Djeu with respectively 39.87 km<sup>2</sup>, 8.44 km<sup>2</sup>, 4.52 km<sup>2</sup>, 1.78 km<sup>2</sup>  
262 and 1.59 km<sup>2</sup>. They contain essentially 40-66 wt.% of alumina that is less than those of Minim-Martap  
263 (45–75wt%) but more than those of Ngaoundal-Ngaoundourou (46-48 wt.%) in the Adamaoua region  
264 (Eno Belinga, 1966; Vicat and Bilong, 1998). The total bauxite reserve of the Bamiléké plateau is still not  
265 quantified. However, some attempts based on (i) thickness data from limited number of pits and (ii)  
266 surface evaluation by contouring have been performed on the Fongo-Tongo and the Doumbouo-Fokoué  
267 spots with 46 million tons (Hiéronymus, 1973) and 9 million tons (Momo Nouazi et al., 2012),  
268 respectively. These values are lower than those of the Adamaoua region of Cameroun. The Bangam spot  
269 revealed by this study with the largest (39.9 km<sup>2</sup>) and richest bauxitic ore (45-66 wt.% alumina) has  
270 unfortunately not been evaluated so far. Further researches on vertical extent of bauxite in this spot are  
271 thus highly recommended here.

272

## 273 **6. Summary and conclusion**

274 This study has suitably combined spatial multisource data to define potential bauxitic laterites  
275 distribution on the Bamiléké plateau, and evaluate the usefulness of including field observations, and  
276 geochemical data processed by statistical method for improving the mineral mapping process. Genetic  
277 criteria and a regolith landform model were successfully used to predict and precisely delineate areas of  
278 bauxite occurrence, thereby highlighting a total bauxitic-rich surface of 56.2 km<sup>2</sup>. The alumina content of  
279 these duricrusts is quite high, but the large spatial distribution into five spots may render their bauxitic  
280 exploitation quite expensive. However, results of this study can be considered as an important input into  
281 the assessment and classification of lateritic ores in Cameroon.

282 At the national-wide level, the bauxitic laterites potential has not yet been fully assessed. Using  
283 the approach developed in this study, the bauxite potential for the entire country could be achieved much  
284 more cheaply than the traditional methods. The whole Cameroon volcanic line with deep weathered and

285 elevated volcanic shields provides most of the useful genetic and geomorphic criteria applicable for such  
286 study.

287

## 288 **Acknowledgement**

289 The financial support for geochemical data of this study was provided by the SCAC (Service de  
290 Coopération et d'Action Culturelle de la France au Cameroun). The geochemical analysis have been  
291 carried out at the Centre Européen de Recherche et d'Enseignement des Géosciences de l'Environnement  
292 (CEREGE), Aix Marseille University, OSU Pytheas, France.

293

## 294 **References**

295 Ballentine, C.J., Lee, D.C., Halliday, A.N., 1997. Hafnium isotopic studies of the Cameroon Line and  
296 new HIMU paradoxes. *Chemical Geology* 139, 111-124.

297 Beauvais, A., Chardon, D., 2013. Modes, tempo, and spatial variability of Cenozoic cratonic denudation:  
298 The West African example. *Geochemistry, Geophysics, Geosystems* 14(5), 1590-1608.  
299 doi:10.1002/ggge.20093.

300 Bildgen, P., 1973. Contribution à l'étude de la genèse et de l'évolution des bauxites karstiques de  
301 Provence: géologie, minéralogie, géochimie des formations bauxitiques des Alpilles. Doctorat  
302 3ème cycle, Paris, 134 pp.

303 Bonham-Carter, G.F., 1994. *Geographic Information Systems for Geoscientists. Modeling with GIS*. First  
304 ed. Pergamon, New York.

305 Boroushaki, S., Malczewski, J., 2008. Implementing an extension of the analytical hierarchy process  
306 using ordered weighted averaging operators with fuzzy quantifiers in ArcGIS. *Computers &  
307 Geosciences* 34(4), 399-410.

308 Boulangé, B., 1984. Les formations bauxitiques latéritiques de Côte d'Ivoire. Les faciès, leur  
309 transformation, leur distribution et l'évolution du modelé. Thèse et Mémoire ORSTOM, 363 pp.

310 Boulangé, B., Ambrosi, J.-P., Nahon, D., 1997. Laterites and Bauxites. In: H. Paquet and N. Clauer  
311 (Editors), Soils and Sediments : mineralogy and geochemistry. Springer Berlin Heidelberg, pp.  
312 49-65

313 Boulangé, B., Bouzat, G., Pouliquen, M., 1996. Mineralogical and geochemical characteristics of two  
314 bauxite profiles, Fria, Guinea Republic. *Mineral Deposita* 31, 432-438.

315 Boulangé, B., Colin, F., 1994. Rare earth element mobility during conversion of nepheline syenite into  
316 lateritic bauxite at Passa Quatro, Minas Gerais, Brazil. *Applied geochemistry* 9, 701-711.

317 Carranza, E.J.M., 2002. Geologically-Constrained Mineral Potential Mapping (Examples from the  
318 Philippines). Ph.D. Thesis, International Institute for Geo-Information Science and Earth  
319 Observation, Enschede, 480 pp.

320 Carranza, E.J.M., 2009. Geochemical anomalies and mineral prospectivity mapping in GIS., *Handbook of*  
321 *exploration and environmental geochemistry* pp. 351.

322 Carranza, E.J.M., Mangaoang, J.C., Hale, M., 1999. Application of mineral exploration models and GIS  
323 to generate mineral potential maps as input for optimum land-use planning in the Philippines.  
324 *Natural Resources Research* 8(2), 165-173.

325 Carranza, E.J.M., van Ruitenbeek, F.J.A., Hecker, C., van der Meijde, M., van der Meer, F.D., 2008.  
326 Knowledge-guided data-driven evidential belief modeling of mineral prospectivity in Cabo de  
327 Gata, SE Spain. *International Journal of Applied Earth Observation and Geoinformation* 10(3),  
328 374-387.

329 Chardon, D., Chevillotte, V., Beauvais, A., Grandin, G., Boulangé, B., 2006. Planation, bauxites and  
330 epeirogeny: One or two paleosurfaces on the West African margin? *Geomorphology* 82, 273-282.  
331 doi:210.1016/j.geomorph.2006.1005.1008.

332 Cheng, Q., Agterberg, F.P., 1999. Fuzzy weights of evidence and its application in mineral potential  
333 mapping. *Natural Resources Research* 8 (1), 27-35.

334 De Araújo, C.C., Macedo, A.B., 2002. Multicriteria Geologic Data Analysis for Mineral Favorability  
335 Mapping: Application to a Metal Sulphide Mineralized Area, Ribeira Valley Metallogenic  
336 Province, Brazil. *Natural Resources Research* 11(1), 29-43.

337 Déruelle, B., Moreau, C., Nkoumbou, C., Kambou, R., Lissom, J., Njonfang, E., Ghogomu, R.T., Nono,  
338 A., 1991. The Cameroon Line: a review. In: A.B. Kampunzu, R.T. Lubala (Eds.), *Magmatism in  
339 extensional structural settings. The Phanerozoic African Plate*. Springer, Berlin, pp. 274-327.

340 Dumort, J.C., 1968. Carte géologique de reconnaissance au 1/500.000. . imprimerie Nationale, D.M.G.  
341 Yaoundé, .

342 Eno Belinga, S.M., 1966. Contribution à l'étude géologique, minéralogique et géochimique des  
343 formations bauxitiques de l'Adamaoua (Cameroun) Doctorat de Troisième Cycle, Université de  
344 Paris, Paris 155 pp.

345 Eno Belinga, S.M., 1968. Etude pétrographique des bauxites de Ngaoundal et de Minim-Martap dans  
346 l'Adamaoua (Cameroun). *Annales de la Faculté des Sciences* 1, 55-68.

347 Eno Belinga, S.M., 1972. L'altération des roches basaltiques et le processus de bauxitisation dans  
348 l'Adamaoua (Cameroun). Doctorat d'Etat, Université Paris, Paris, 571 pp.

349 FAO-ISRIC, 2006. *World Reference Base for Soil Resources* FAO, Rome.

350 Grandin, G., Thiry, M., 1983. Les grandes surfaces continentales tertiaires des régions chaudes.  
351 Succession des types d'altération. *Cahier ORSTOM, série Géologie* 13(1), 3-18.



352 Guha, A., Singh, V.K., Parveen, R., Vinod Kumar, K., Jeyaseelan, A.T., Dhanamjaya Rao, E.N., 2013.  
353 Analysis of ASTER data for mapping bauxite rich pockets within high altitude lateritic bauxite,  
354 Jharkhand, India. *International Journal of Applied Earth Observation and Geoinformation* 21,  
355 184-194.

356 Harris, J.R., Lemkow, D., Jefferson, C., Wright, D., Falck, H., 2008. Mineral Potential Modelling for the  
357 Greater Nahanni Ecosystem Using GIS Based Analytical Methods. *Natural Resources Research*  
358 17(2), 51-78.

359 Harris, J.R., Wilkinson, L., Heather, K., Fumerton, S., Bernier, M.A., Ayer, J., Dahn, R., 2001.  
360 Application of GIS processing techniques for producing mineral prospectivity maps - a case  
361 study: mesothermal Au in the Swayze Greenstone Belt, Ontario, Canada. *Natural Resources*  
362 *Research* 10(2), 91-124.

363 Hiéronymus, B., 1973. Etude minéralogique et géochimique des formations bauxitiques de l'ouest  
364 Cameroun. Doctorat 3e Cycle, Univ. Paris VI, Paris, 98 pp.

365 Hodgson, C.J., 1990. Uses (and abuses) of ore deposit models in mineral exploration. *Geoscience Canada*  
366 17(2), 79-89.

367 ITC ILWIS Unit, 2001. ILWIS 3.0 Academic user's guide. ITC, Enschede, NL, pp. 520.

368 Jones, A., Breuning-Madsen, H., Brossard, M., Dampha, A., Deckers, J., Dewitte, O., Gallali, T., Hallett,  
369 S., Jones, R., Kilasara, M., Le Roux, P., Micheli, E., Montanarella, L., Spaargaren, O.,  
370 Thiombiano, L., Van Ranst, E., Yemefack, M., Zougmor, R., (eds.), 2013. *Soil Atlas of Africa*.  
371 European Commission, Publications Office of the European Union, Luxembourg. 176 pp.

372 Kagou Dongmo, A., Nkouathio, D., Pouclet, A., Bardintzeff, J.-M., Wandji, P., Nono, A., Guillou, H.,  
373 2010. The discovery of Late Quaternary basalt on Mount Bambouto: implications for recent

374 widespread volcanic activity in the southern Cameroon Line. *Journal of African Earth Sciences*  
375 57, 96-108.

376 Kwekam, M., Liégeois, J.P., Njonfang, E., Affaton, P., Hartmann, G., 2010. Nature, Origin and  
377 Significance of the Fomopéa Pan-African High-K Calc-alkaline Plutonic Complex in the Central  
378 African Fold Belt (Cameroon) *Journal of African Earth Sciences* 57, 79-95.

379 Maignien, R., 1966. *Compte rendu de recherche sur les laterites*. Col. Rech. Rers. Nat. UNESCO, Paris 4.

380 Marzoli, A., Renne, P.R., Piccirillo, E.M., Francesca, C., Bellieni, G., Melfi, A.J., Nyobe, J.B., N'ni, J.,  
381 1999. Silicic magmas from the continental Cameroon volcanic line (Bambouto and Ngaoundéré):  
382  $^{40}\text{Ar}/^{39}\text{Ar}$  dates, petrology, Sr-Nd-O isotopes and their petrogenetic significance. *Contrib.*  
383 *Mineral. Petrol.* 135, 133-150.

384 Momo Nouazi, M., Tematio, P., Yemefack, M., 2012. Multiscale organization of the Doumbouo-Fokoué  
385 Bauxites Ore Deposits (West Cameroun): Implication to the Landscape Lowering. *Open Journal*  
386 *of Geology* 2, 14-24.

387 Morin, S., 1985. *Cuirasses et reliefs de l'ouest Cameroun*, Laboratoire de géomorphologie du  
388 CEGET/CNRS, 33405 Talence, France.

389 Nicolas, J., Eno Belinga, S.M., 1969. Contribution à l'étude de l'origine et de l'évolution des bauxites de  
390 l'Adamaoua (Cameroun). *C. R. Ac. SC. Paris, série D*, 268, 1157-1160.

391 Nkouathio, D.G., 2006. Evolution tectono-magmatique et volcanologique de la Ligne du Cameroun:  
392 comparaison d'un volcanisme de graben (plaine de Tombel) et d'un volcanisme de horst (monts  
393 Bambouto). Thèse Doctorat Thesis, Université Yaoundé-1, Yaounde, Cameroun, 231 pp.

394 Nkouathio, D.G., Kagou, D.A., Bardintzeff, J.M., Wandji, P., Bellon, H., Pouclet, A., 2008. Evolution of  
395 volcanism in graben and horst structures along the Cenozoic Cameroon Line (Africa):  
396 implications for tectonic evolution and mantle source composition. *Min. Pet.* 94, 287-303.

397 Ntép Gweth, P., 2009. Ressources minérales des arrondissements de la région de l'Ouest. Extrait de la  
398 carte thématique de ressources minérales du Cameroun sur un fond géologique (2001).

399 Nyobe, J.B., 1987. A geological and geochemical study of the Fongo-Tongo and areally related bauxites  
400 deposits, Wersten Highlands, Republic of Cameroun. PhD thesis, 352 pp.

401 Pedro, C., 1968. Distribution des principaux types d'altérations à la surface du globe. Présentation d'une  
402 esquisse géographique. *Revue Géogr. Phys. Géol. Dyn.* 10(5), 457-470.

403 Reeves, C.V., Westerhof, A.B., Botman, L.G., Dessauvagie, T.F.J., Dijkstra, S., 1990. Systematic mineral  
404 resource development in the '90s and the next century: new techniques, old challenges. *ITC*  
405 *Journal* 2, 92-101.

406 Riis, F., Fjeldskaar, W., 1992. On the magnitude of the late Tertiary and Quaternary erosion and its  
407 significance for the uplift of Scandinavia and the Barents sea. In: R.M. Larsen, H. Brekke, B.T.  
408 Larsen, E. Talleras (Eds.), *Structural and tectonic modeling and its application to petroleum*  
409 *geology*. NPF Special Publications 1, Elsevier Amsterdam, pp. 163-185.

410 Robinove, C.J., 1989. Principles of logic and the use of digital geographic information systems. In: W.J.  
411 Ripple (Ed.), *Fundamentals of Geographic Information Systems, a Compendium*. American  
412 Society for Photogrammetry and Remote Sensing, pp. 112-124.

413 Segalen, D., 1967. Les sols et la géomorphologie du Cameroun *Cahier ORSTOM, Sér. Pédologie* 5(2),  
414 137-187.

415 Soler, J.M., Lasaga, A.C., 2000. The Los Pijiguaos bauxite deposit (Venezuela): A compilation of field  
416 data and implications for the bauxitization process *Journal of South American Earth Sciences* 13,  
417 47-65.

418 Tardy, Y., 1993. *Péetrologie des latérites et des sols tropicaux*. Masson, Paris.

419 Tematio, P., 2005. Etude cartographique et pétrographique des sols à caractères ferralitiques et  
420 andosoliques dans les monts Bambouto (Ouest Cameroun): influence de la nature lithologique et  
421 des facteurs du milieu sur la nature et la distribution des sols en régions de montagne tropicale  
422 humide. Doctorat d'Etat Thesis, Univ. Yaoundé I, Yaounde, 251 pp.

423 Tematio, P., Fritsch, E., Hodson, M.E., Lucas, Y., Bitom, D., Bilong, P., 2009. Mineral and geochemical  
424 characterization of a leptic-aluandic soil and athapto-aluandic-ferralsol developed on trachytes in  
425 Mount Bambouto (Cameroon volcanic line). *Geoderma* 152, 314-323.

426 Tematio, P., Kengni, L., Bitom, D., Hodson, M., Fopoussi, J.C., Leumbe, O., Mpakam, H.G., Tsozué, D.,  
427 2004. Soils and their distribution on Bambouto volcanic mountain, West Cameroon highland,  
428 Central Africa. *Journal of African Earth Sciences*. 39, 447-457.

429 Theodossiou, N., Latinopoulos, P., 2006. Evaluation and optimization of ground water observation  
430 network using the Kriging methodology. *Environmental modeling and software* 21, 991-1000.

431 Thiart, C., De Wit, M., 2000. Linking spatial statistics to GIS: exploring potential gold and tin models of  
432 Africa. *South African Journal of Geology* 103(3-4), 215-230.

433 Thole, U., Zimmermann, H.-J., Zysno, P., 1979. On the suitability of minimum and product operators for  
434 intersection of fuzzy sets. *Fuzzy Sets and Systems* 2(3), 167-180.

435 Tsopjio Jiomeneck, S.P., Tematio, P., Wilson, A., Yemefack, M., 2011. Andosolization of Soils on a  
436 Strombolian Cone at Mount Bambouto, Cameroon. *Open Journal of Soil Science* 1, 97-105.

437 Varnes, D.J., 1974. The logic of geological maps, with reference to their interpretation and use for  
438 engineering purposes. United States Geological Survey Professional Paper 837.

439 Vicat, J.-P., Bilong, P., 1998. Géosciences au Cameroun. Presses Universitaires de Yaoundé.

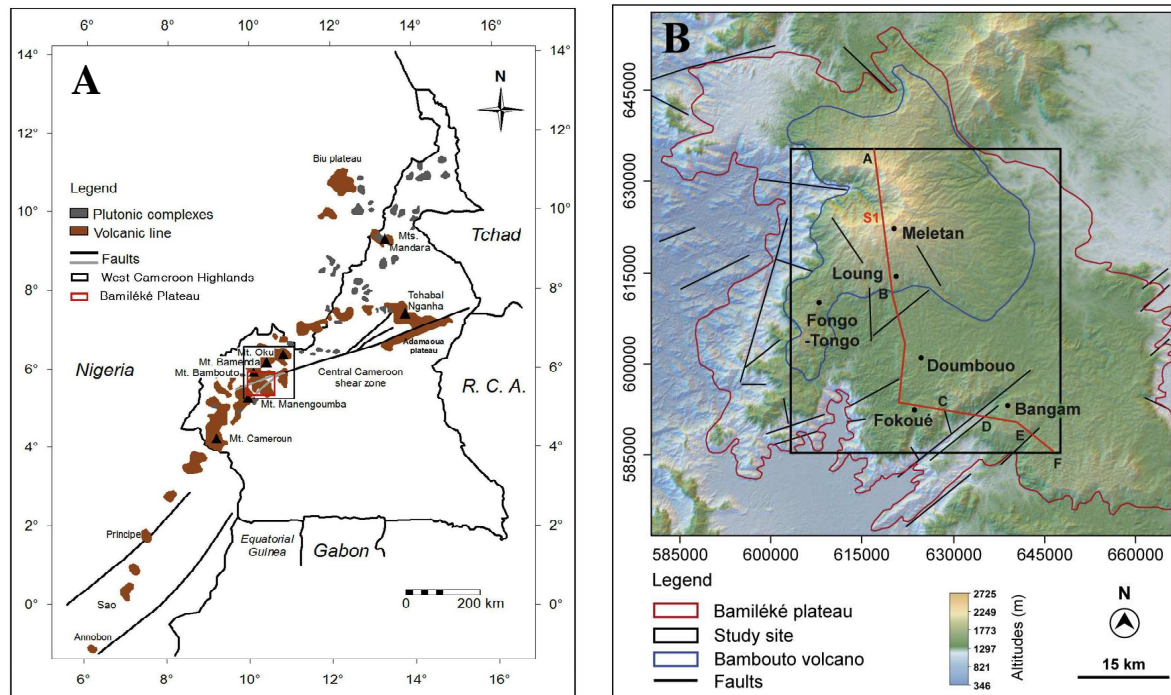
440 Zadeh, L.A., 1965. Fuzzy sets. *IEEE Information and Control* 8 (3), 338-353.

441

442 Table 1. Alumina (wt.%) of diricrusted laterites on the Bamiléké Plateau

<b>Lower surface</b>		<b>Upper surface</b>							
Doumbouo-Fokoué		Fongo-Tongo		Bangam		Loung		Djeu	
Sample	Al <sub>2</sub> O <sub>3</sub> (wt%)	Sample	Al <sub>2</sub> O <sub>3</sub> (wt%)	Sample	Al <sub>2</sub> O <sub>3</sub> (wt%)	Sample	Al <sub>2</sub> O <sub>3</sub> (wt%)	Sample	Al <sub>2</sub> O <sub>3</sub> (wt%)
DF1	31.3	FO1	50.8	BA1	51.1	LO1	57.3	DJ1	22.3
DF2	35.1	FO2	59.7	BA2	47.1	LO2	39.1	DJ2	27.2
DF3	52.6	FO3	34.0	BA3	48.4	LO3	54.7	DJ3	28.9
DF4	38.7	FO4	43.1	BA4	38.4	LO4	44.3	DJ4	47.3
DF5	37.6	FO5	44.4	BA5	38.3	LO5	53.7	DJ5	40.0
DF6	42.0	FO6	47.2	BA6	60.3	LO6	46.9	DJ6	35.2
DF7	44.5	FO7	49.4	BA7	60.4	LO7	54.9	DJ7	38.4
DF8	28.7	FO8	51.6	BA8	59.7				
DF9	35.9	FO9	48.2	BA9	46.8				
DF10	36.0	FO10	37.4	BA10	43.5				
DF11	35.0	FO11	44.0	BA11	42.8				
DF12	47.5	FO12	49.8	BA12	40.0				
DF13	49.5	FO13	57.5	BA13	47.3				
DF14	36.0	FO14	44.9						
DF15	33.3	FO15	50.1						
DF16	37.7	FO16	49.9						
DF17	13.8	FO17	39.3						

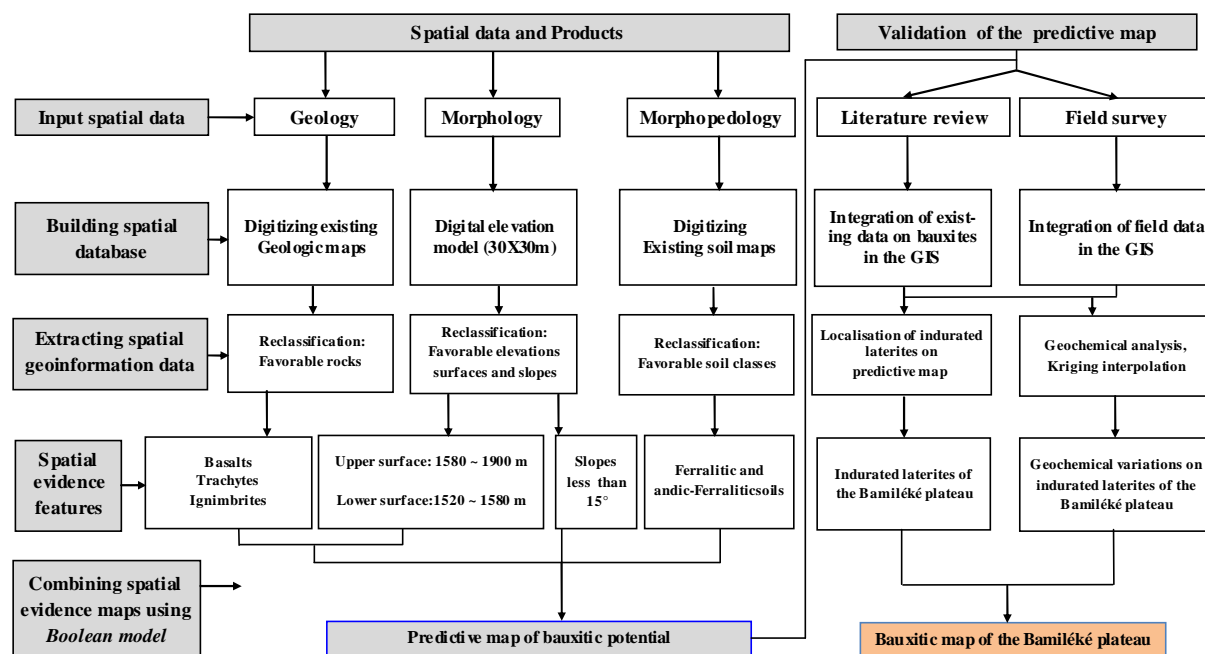
443



444

445 Figure 1. A: Localization and structure of the Cameroon volcanic line (from Ballentine et al., 1997; and Ngako et  
 446 al., 2006); B: morphology of the Bamiléké plateau. Letters A to F mark the major morphological changes  
 447 along the cross section in figure 4.

448

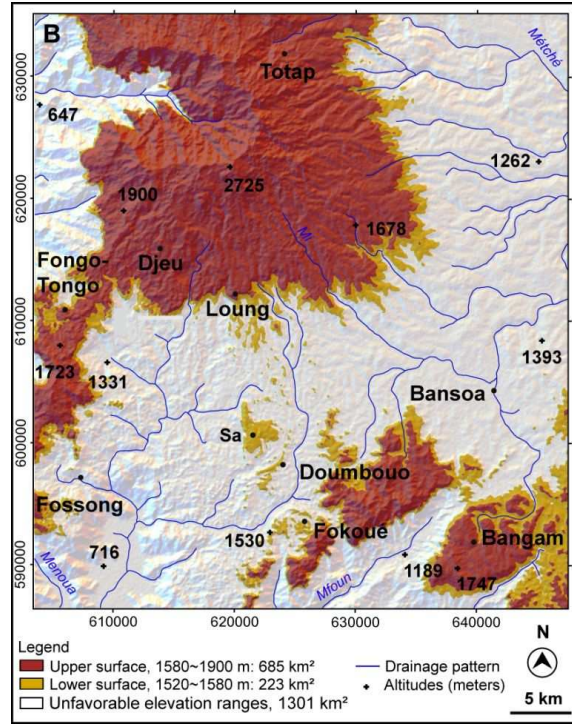
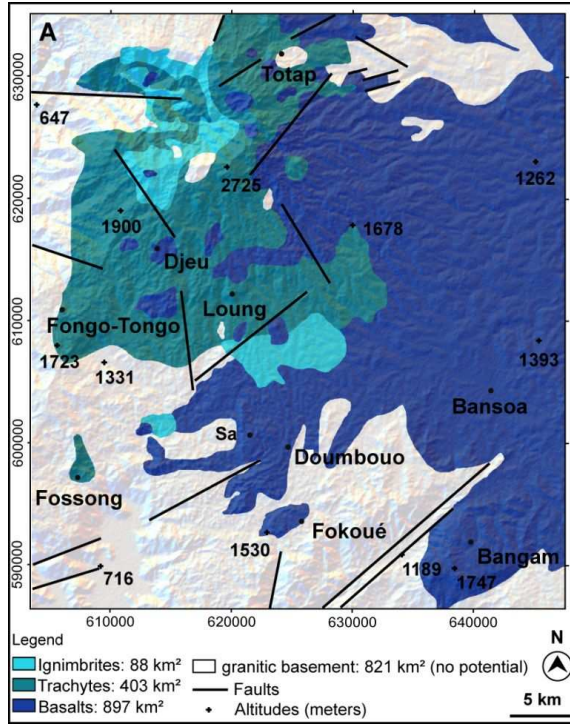


449

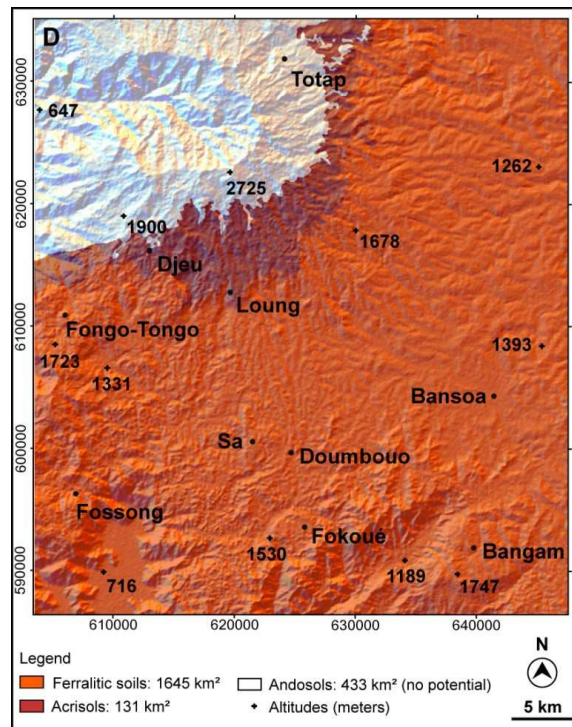
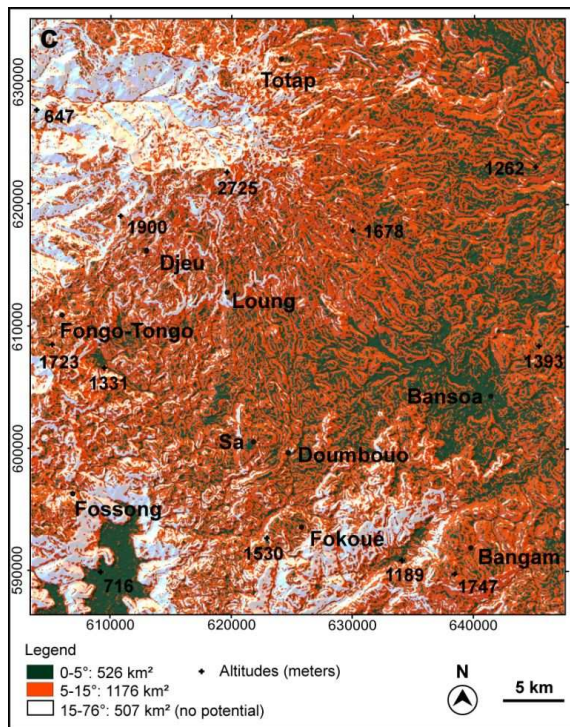
450 Figure 2. Methodology applied to undertake geologically constrained mapping of the Bamiléké plateau bauxites

451

452



453



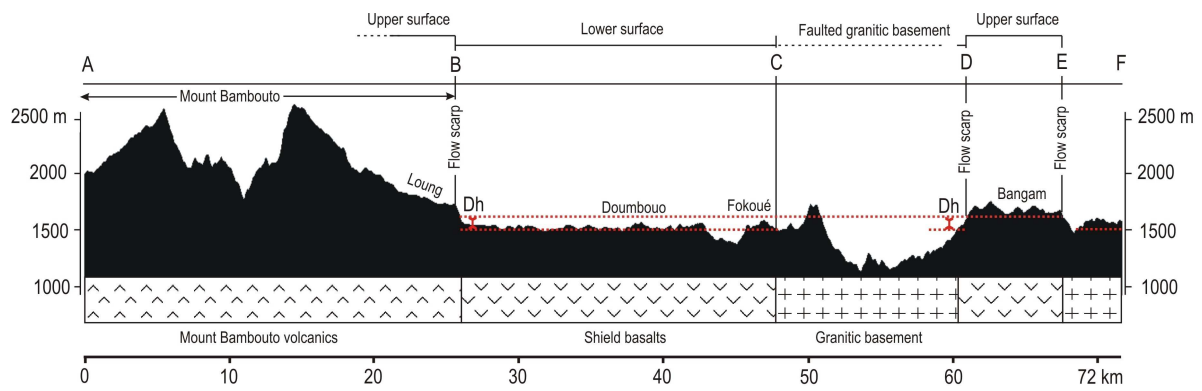
454

Figure 3. Favorable constraints maps. A: rocks; B: elevation ranges; C: slopes; D: soil

455



456



457

458

Figure 4. Cross section showing the vertical and lateral distribution of lateritic surfaces. Section S1 on figure 1B

459

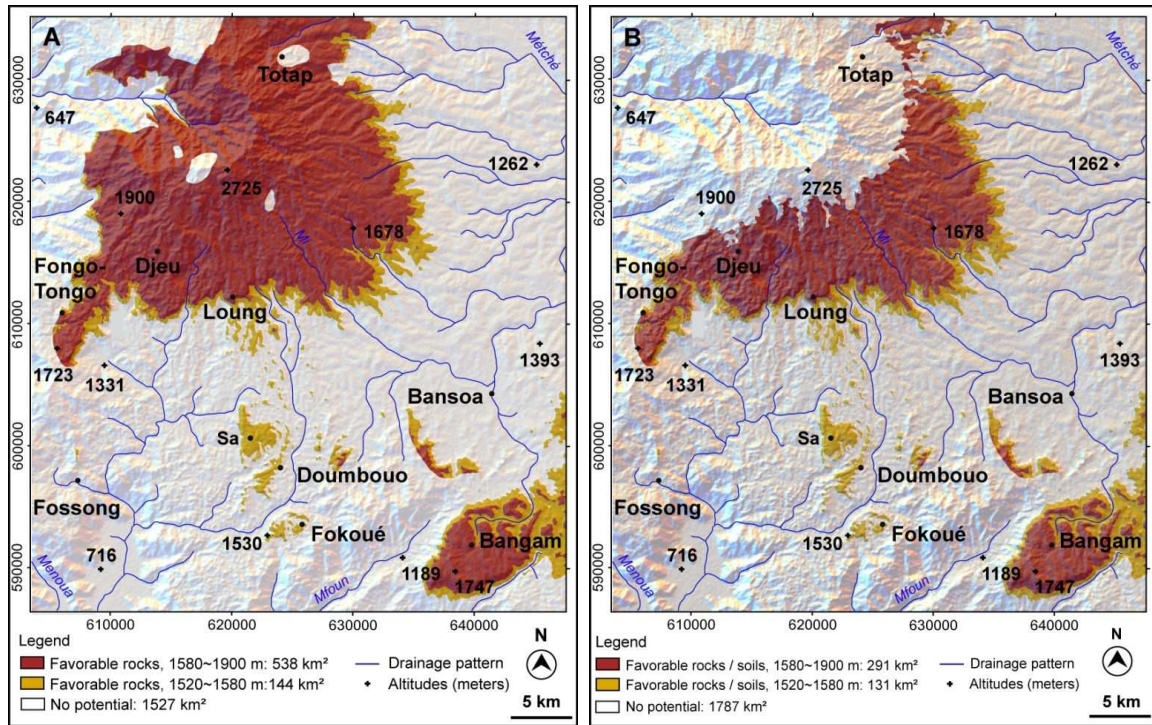


460

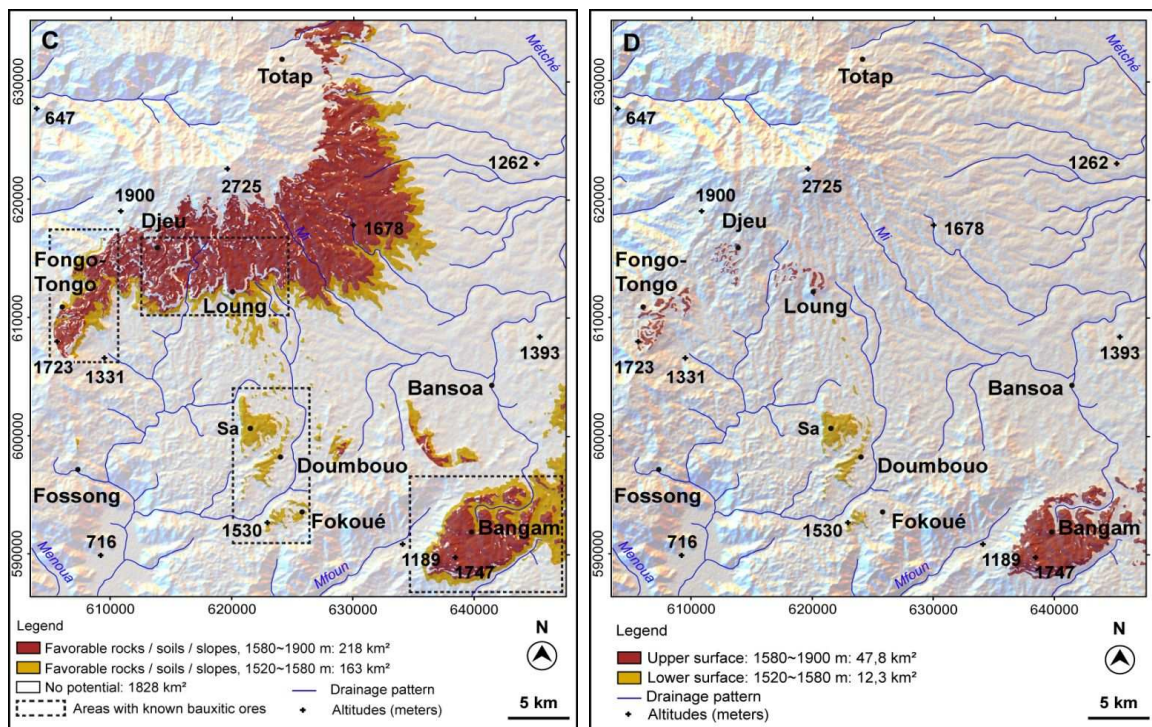
461 Figure 5. Morphological distribution of duricrust on the Bamiléké plateau. A: continuous duricrust on flat  
462 interfluves; B: steep slope limiting flat duricrust on the top; C: convex slope showing evidence of  
463 duricrust dismantling

464

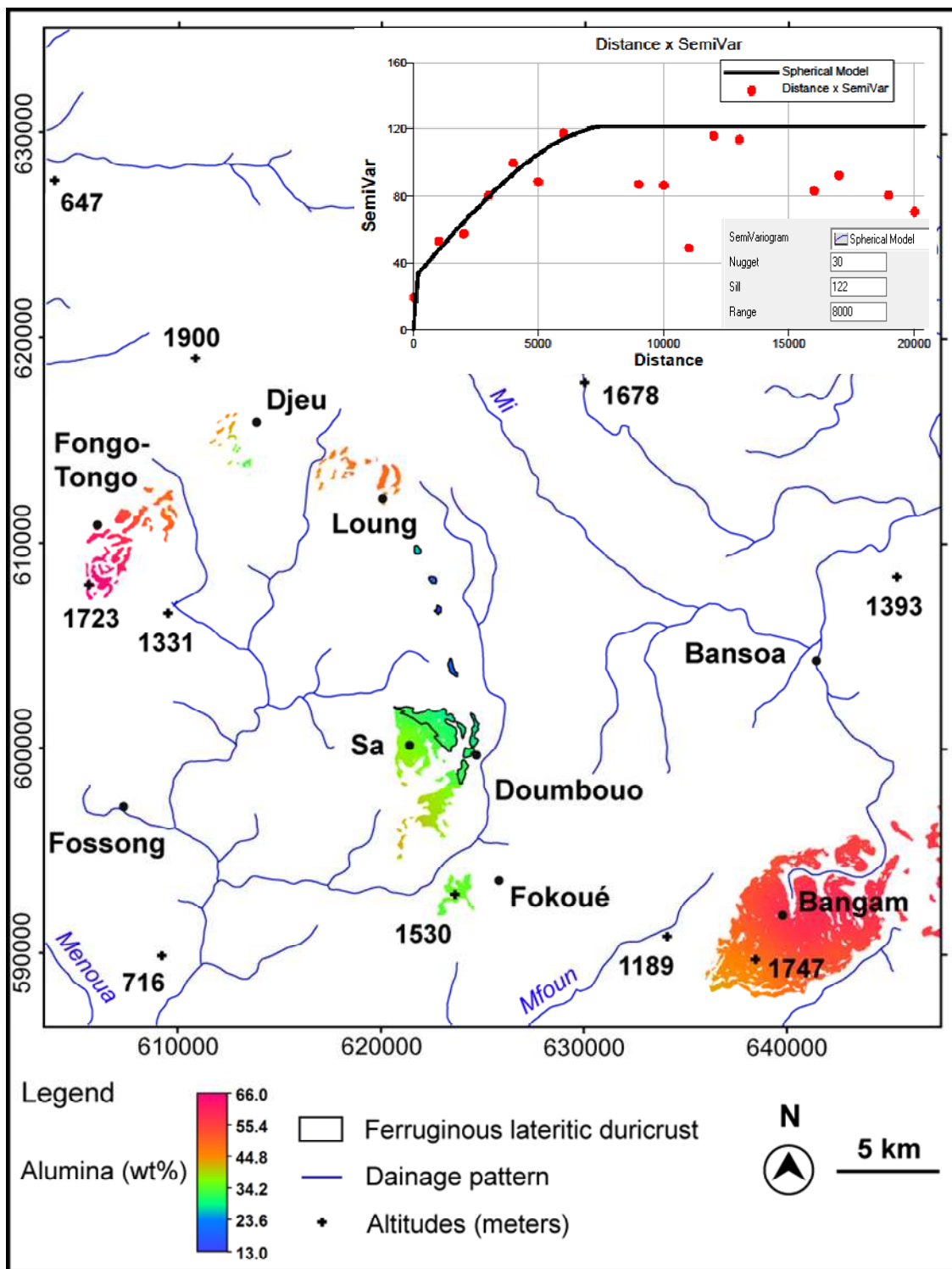
465



466



467 Figure 6. Potential maps and field validation results. A: favorable elevation ranges constrained with favorable rock  
 468 types; B: A constrained with favorable soil classes; C: B constrained with favorable slopes; D: map of  
 469 indurated laterites of the Bamiléké plateau.



470

471 Figure 7. A: Semi-variogram model; B: map showing the distribution of alumina percentages on indurated laterites  
 472 of the Bamiléké plateau